Ethanolamine improves colonic barrier functions and inflammatory immunoreactions via shifting microbiome dysbiosis

Jian Zhou[1,3], Xia Xiong[1#], Dan Wan[1], Hongnan Liu[1], Yirui Shao[1,3], Yuliang Wu[1], Xiali Huang[1], Chanfeng Peng[1], Pan Huang[1], Lijun Zou[1,4], Yulong Yin [1, 2, 3,4]

1. National Engineering Laboratory for Pollution Control and Waste Utilization in Livestock and Poultry Production; Key Laboratory of Agro-Ecological Processes in Subtropical Region, Institute of Subtropical Agriculture, Chinese Academy of Sciences; Hunan Provincial Engineering Research Center for Healthy Livestock and Poultry Production; Scientific Observing and Experimental Station of Animal Nutrition and Feed Science in South-Central, Ministry of Agriculture, Changsha, Hunan 410125, China;

2. Hunan International Joint Laboratory of Animal Intestinal Ecology and Health, Laboratory of Animal Nutrition and Human Health, College of Life Sciences, Hunan Normal University, Changsha, Hunan, 410081, China;

3. University of Chinese Academy of Sciences, Beijing, China.

4.Laboratory of Basic Biology, Hunan First Normal University, Changsha 410205, China.

 # Address correspondence to Xiong Xia, xx@isa.ac.cn & Yin Yulong,yinyulong@isa.ac.cn

Abstract

Ethanolamine(EA) often occurs at a relatively high concentration within the inflamed gut of IBD patients.To investigate the role of EA in colonic inflammation and host-microbiome dysbiosis, thirty-six ICR mice were treated with 3% DSS for a week to generate acute intestinal inflammation and then supplied with 0μM, 500μM (LowEA), and 3000 μM (HighEA) in drinking water for two weeks, after that,16s RNA sequencing was applied in characterizing the changes in colonic microbiota driven by different EA levels. An inflamed colonic organoid model via 3% DSS treatment was also established for further verification of these in vivo findings.EA significantly reduced proximal colonic crypt depth but increased distal colonic villus height in HighEA group. The protein and mRNA expression of occludin and Reg3β, BD1, BD2, and MUC2were significantly up-regulated in EA treated groups. EA decreased mucosal inflammation-related cytokines levels (IL1, IL6, IL17, TNFα, and INFγ) and increased the significantly increased concentration of sIgA. Serum aspartate aminotransferase and alanine aminotransferase were significantly down-regulated in the highEA group. EA increased the relative abundance of *Blautia, Roseburia, Lactobacillus, Faecalibaculum, Candidatus_Saccharimonas, Alloprevotella,* and *Lachnoclostridum*.and thus microbial metabolic pathways including *Oxidative phosphorylation, Lipopolysaccharide biosynthesis, Arginine and proline metabolism, Folate biosynthesis,* and *Biotin metabolism* were more abundant in LowEA group than those in control. EA up-regulated the protein or mRNA expression of TLR4/MyD88 in colonic tissues and the DSS-treated colonic organoid model. This study firstly demonstrated that ethanolamine in altering host-microbiome dysbiosis, which may provide new insights into the role of dietary lipids in IBD.

Keywords: CDP-ethanolamine, Inflammatory bowel diseases, Gut microbiota, host-microbial interactions

Importance

Inflammatory bowel disease (IBD) affects ~3.1 million people in the USA and is increasing in incidence worldwide. IBD pathogenesis has been associated with gut microbiome dysbiosis characterized as a decrease in gut microbial diversity. Extensive works have demonstrated the

roles of dietary fiber, short-chain fatty acids, and aromatic amino acids in altering the composition of gut microbiota to restore immune homeostasis and alleviate inflammation via diverse mechanisms in IBD. However, little is known about essential sphingolipids like ethanolamine (EA), an essential compound in the CDP-ethanolamine pathway for phosphatidylethanolamine (PE) in both intestinal cells and bacteria. PE synthesis deficiency can ultimately result in a loss of membrane integrity and metabolic disorders in IBD.Our results demonstrate that ethanolamine could improve colonic barrier functions and inflammatory immunoreactions via shifting microbiome dysbiosis, which provides new insights into the role of dietary lipids in IBD.

1.Introduction

Nutrient signals, microbiome dysbiosis, and host immunoreactions have a pivotal role in the development of inflammatory bowel diseases (IBD) and colorectal cancer[1-4]. The gastrointestinal tract not only acts as the primary site of food digestion and nutrition absorption but also provides an essential interface for the interactions of gut microbiota and immune systems[5]. Dramatic alterations in the composition of gut microbiota and intestinal barrier dysfunction have been found in IBD Patients[3, 6].Nutrient signals including gut microbial-derived metabolites, aromatic amino acids, short-chain fatty acids and activate compounds can directly impact the establishment of the tumor-associated microenvironment and contribute to host-microbial interactions in the progress of the colorectal cancer[3-4]. Extensive works have demonstrated the roles of L-arginine[7] and tryptophan[8], and short-chain fatty acids like butyrate[9] and acetate[10] in altering host-microbial interactions to restore gut homeostasis and alleviate intestinal inflammation through diverse mechanisms[3]. However, little is known about essential sphingolipids like ethanolamine (EA), an essential compound in the CDP-ethanolamine pathway for phosphatidylethanolamine (PE) synthesis[11]. PE synthesis deficiency can ultimately result in a loss of membrane integrity and metabolic disorders in inflammatory diseases[10, 12]. The gastrointestinal tract keeps a physiological concentration of EA at 1~2mM via daily diet intake and internal recycling of PE to maintain intestinal metabolic homemstatsis[13].

IBD patients consistently suffered from chronic inflammation and held more opportunities to develop cancer[14]. Lipid-mediated host-microbial interactions in metabolism and immune reactions are implicated in chronic inflammatory diseases like IBD[15]. Ethanolamine has been detected at a relatively high concentration within the inflamed gut of both IBD patients and rodent models as the hydrolysate of PE[16-17]. Ethanolamine can be utilized by both intestinal epithelial cells[11] and bacteria like *Enterococcus faecalis*[18] that hold the EA utilization (*eut*) genes via the CDP-EA pathway[10], which confers it with the potential role in mediating the cross-talk between the intestinal epithelium and gut microbiota. A recent study highlighted that EA could promote the mesenchymal-to-epithelial transitions via a CDP-EA-Pebp1 dependent manner that ultimately leads to NF-κB inhibition[11]. Ethanolamine has been associated with the pathogenesis of *eut* pathogens such as *Salmonella*[16] and enterohemorrhagic *Escherichia coli* (EHEC)[17] that have been reported to promote colorectal carcinogenesis and tumor formation[2-3]. For instance, several studies have demonstrated that *S. Typhimurium* can sidestep nutritional competition with commensal bacteria by utilizing EA in inflamed gut[16, 19-20]. Toll-like receptors (TLRs) have a vital role in mucosal immune responses to gut bacteria, and the TLR4 expression was always dramatically up-regulated in the intestines of IBD patients[21]. Myeloiddifferentiationfactor (MyD) 88 holds its essential role in the regulation of innate gut immunity, and it is the direct downstream of TLRs and

cytokine receptors[22]. Nutrient signals such as peptidoglycan and lipopolysaccharide can activate TLR4-MyD88 dependent or independent pathways to regulate the expression of antimicrobial proteins like the Reg3 protein family that ultimately reprogramme the gut microbiome in IBD[23-24]. However, The role of EA on TLR4/MyD88 signaling to restore microbiome dysbiosis under inflammatory conditions remains unknown.

Our previous study has preliminarily demonstrated that 500~1000 mM supplementation of EA could alleviate weaning stress via re-programing gut microbiota[13]. To investigate the potential role of Etn as a nutrient signal in microbial-host interactions, the impact of Etn on colonic morphology, antimicrobial protein expression, inflammation-related cytokines, serum indicators, and gut microbiome were investigated.

2. Materials and methods

2.1 Animals and Experimental Design

All experiments were approved by the Animal Care and Use Committee of the Institute of Subtropical Agriculture, Chinese Academy of Sciences[25]. Thirty-six male ICR mice (three-week-old) were obtained from the SLAC Laboratory Animal Central (Changsha, China). All mice were housed under standard conditions, in pathogen-free colonies (temperature, 22 ± 2 °C; relative humidity, 50 ± 5%; lighting cycle, 12 h/d), with free access to food and water. Intestinal colitis was induced in all mice by administration of 3% DSS (MP Biomedicals Shanghai, Co., Ltd. molecular weight=165.192 g/mol) in drinking water for seven days as previously described[26]. After that, thirty mice with colitis were obtained and randomly assigned into three groups (n =8) including the control group (Control) without EA (EA, Sigma-Aldrich,CAS141-43-5) supplements and two treatment groups that were supplemented with 500μM EA (LowEA) and 3000 μM EA(HighEA) in drinking water for two weeks(Figure 1A).

2.2 Colonic crypt isolation and DSS-treated organoid culture

Mouse colonic crypts were harvested from three male 8-week-old ICR mice and cultured, as previously described[27]. In brief, 3 cm segments of the colon were minced and washed with cold DPBS(Stem cell,cat#37350) for 15~20 times until the supernatant is clear. The tissue pieces were digested in Gentle cell dissociation reagent(Stem cell,cat#07174) for 20~30min on a rocking platform at 20 rpm. The crypt compartment was collected by centrifugation and then washed twice with DMEM/F12 media(Stem cell,cat#36254). Then crypt pellets were resuspended with 25μl matrigel matrix (Corning,cat#356231) and 25μl medium per well and plated onto a 24-well tissue culture plated with complete mouse organoid growth medium(Stemcell, cat#06000) 10 μM Y-27632 ROCK inhibitor(Stem cell,cat#72302). After a week, mature colonic organoids were resuspended with matrigel matrix and medium as well as 3% DSS (MP Biomedicals,cat# 02160110) to form matrigel domes(Figure 8A) and cultured as previously reported methods[28].

2.3 Morphological analysis

Cross-sections of tissue samples from each group were preserved in 4% formaldehyde, and glutaraldehyde mixing fixative was prepared using standard paraffin embedding techniques. Then samples were sectioned at 5μm thickness and were stained with hematoxylin and eosin as previously described[29]. Villus height (VH) and crypt depth (CD) were measured under a light

133 microscope at 40× magnification using an image processing and analysis system (Leica Imaging
134 Systems, Cambridge, UK). A minimum of 10 well-oriented, intact villi was measured from the
135 crypt mouth to the villus tip and all measurements were made in 10 μm increments, and the count
136 was repeated three times for each section per sample.
137
138 **2.4 Immunohistochemistry Assay**
139 Tissue samples from colons were cut into 4-μm sections and processed for
140 immunohistochemical staining as described[30]. And then, these samples were incubated with a
141 primary antibody anti-occludin(Abcam,cat#ab31721) overnight at 4◦C and then with
142 poly-horseradish peroxidase-conjugated occludin for 60min at 22±4◦C.Subsequently, the
143 avidin-biotin-peroxidase complex and the substrate 3,3′-diaminobenzidine were applied for 2min
144 and the samples were analyzed.
145
146 **2.5 Enzyme-Linked Immunosorbent Assay**
147 Levels of IL1, IL6, TNFα,IL17,INFγ,sIgA,IL10, and IL22 in colonic segments were
148 measured using ELISA kits according to the manufacturer's instructions as previous studies[13]. The
149 ELISA kits are from (Meimian,Yutong Biological Technology Co., Ltd,Jiangsu,China). Briefly,
150 supplied diluent buffer in the kits was used to dilute standards and serum samples. Next, 100 μL of
151 the sample or standard in duplicate was added to the wells of a microtitre plate precoated with
152 wash antibody. Diluent buffer was applied as a negative control. The plates were incubated for 2
153 hours at 37°C. After incubation, 100 μL of biotin-antibody was added to each well after removing
154 the liquid and incubated for 1 hour at 37°C. All wells were washed three times, with 200 μL
155 volume of wash buffer. Next, 100 μL horseradish peroxidase-avidin was added to each well for 1
156 hour at 37°C. After a final wash, 90 μL of the supplied TMB substrate was added and incubated
157 for thirty minutes in the dark at 37°C. The reaction was stopped with 50 μL of the supplied stop
158 solution, and absorbance was measured at 450 nm with a spectrophotometer.
159
160 **2.6 Serum biochemical analysis**
161 Serum levels of total bile acid(TBA) were detected by the fully automatic biochemical
162 analyzer(Shenzhen Mindray, BS-190), as described in our previous studies[25]. Serum aspartate
163 aminotransferase (AST), alanine aminotransferase (ALT) and dual amine oxidase(DAO) were
164 determined via commercial kits, and all determinations were done in triplicate and performed
165 according to the manufacturer's instructions[25].
166
167 **2.7 Quantifications Real-Time PCR**
168 Total RNA of jejunal mucosa was extracted using TRIZOL reagent (Invitrogen, Carlsbad,
169 CA). The first-strand cDNA was then synthesized using a reverse transcription kit (TaKaRa,
170 Dalian, China) following the manufacturer's instruction, as described in our previous study[29].
171 qPCR was performed using primers shown in the supplemental materials (Sup_Table 1). Briefly, 1
172 μL cDNA template was added to a total volume of 10 μL assay solution containing 5 μL SYBR
173 Green mix,0.2 μL Rox, 3 μL deionized H2O, and 0.4 μL of each of the forward and reverse
174 primers. The comparative Ct value method was used to quantitate mRNA expression relative to
175 β-actin. All samples were run in triplicate and the average values were calculated.

176 **2.8 Western Blot Analysis**

Total proteins from intestinal tissues were extracted with a commercially available kit using lysis buffer containing 1‰ DTT, 5‰ PMSF and 1‰ protease inhibitor (KeyGEN BioTech, Nanjing, China). Following intermittent vortexing for 20 min on ice, samples were centrifuged at 13,000 rpm for 15 min at 4 °C. Protein content was determined using the BCA assay (Pierce Biotechnology, Rockford, IL, USA), and Western blotting analysis was performed. Briefly, 20 μg protein per lane was separated by SDS-PAGE and blotted onto nitrocellulose membranes. Primary antibody against occluding (Abcam,cat#ab31721),anti-TLR4(Abcam,cat#13556) and anti-MyD88(Abcam,cat#133739) and recombinant anti-beta actin antibody (Abcam,cat#ab115777) were incubated with the membrane overnight at 4 °C. After incubating overnight with the secondary antibody, the membrane was exposed to EZ-ECL (Biological Industries, Cromwell, CT, USA) for protein band detection, and all original images of WB results could be found in supplemental materials(Sup_Figure1).

2.9 Microbial sequencing of colon contents

Total bacterial DNA from approximately 0.25 g of colon contents was extracted using a QIAamp DNA Stool Mini Kit (Qiagen, Hilden, Germany) according to the manufacturer's instructions as described[13]. The diversity and composition of the bacterial community were determined by high-throughput sequencing of the microbial 16S rRNA genes. The V4 hypervariable region of the 16S rRNA genes was PCR amplified using 515F: 5′-GTGCCAGCMGCCGCGGTAA-3′ and 806R: 5′-GGACTACHVGGGTWTCTAAT-3′ primers, Illumina adaptors, and molecular barcodes. Paired-end sequencing was performed on the Illumina HiSeq 2500 platform (Novogene, Beijing, China) to obtain raw 16s data. The assembled HiSeq sequences obtained by this research were submitted to the NCBI's Sequence Read Archive with project ID: PRJNA551369 for open access.

2.10 Bioinformatic analysis and metagenomic predictions

Raw 16S data sequences The first-strand before being screened and assembled using the QIIME (v1.9.1) and FLASH software packages as previously described[25]. UPARSE (v7.0.1001) was used to analyze high-quality sequences and determine OTUs. Subsequently, high-quality sequences were aligned against the SILVA reference database (https://www.arb-silva.de/) and clustered into OTUs at a 97% similarity level using the UCLUST algorithm (https://drive5.com/usearch/manual/uclust_algo.html). Each OTU was assigned to a taxonomic level with the Ribosomal Database Project Classifier program v2.20 (https://rdp.cme.msu.edu/), as previously reported[13]. Functional metagenomes of all samples were predicted using Tax4Fun R packages(http://tax4fun.gobics.de)[31]. Further statistical interrogation and graphical depictions of microbiome data were performed by R software (v3.6.0) and related packages.

2.11 Statistical Analysis

Data were analyzed using the General Linear Model (GLM) procedure in SAS (SAS Institute Inc., Cary, NC) to identify significant treatment effects and interactions. All data were presented as Least Squares means plus pooled SEM. The Tukey multiple comparison tests were used to evaluate the differences among the treatments. Probability values ≤ 0.05 were taken to indicate statistical significance.

3. Results

3.1 Impacts of ethanolamine treatment on body weight and colonic morphology

There were no differences in the BW, ADF, and water intake among the three groups (**Figure1** C-D). Compared with control group, Etn decreased the proximal colonic crypt depth ($P < 0.0001$, Figure1 F-H) and increased villus/crypt ratio ($P < 0.0001$). Meanwhile, EA significantly increased the villus height and villus/crypt ratios of distal colon ($P < 0.05$).

3.2 Ethanolamine altered the composition of colonic microbiota

Microbial diversity indicators (Shannon and Simpson)were significantly in the low EA treated group than the control group ($P < 0.0001$; Figure 2 A&B). Besides, microbial abundance represented by Chao1 ($P = 0.014$, Figure2 C) and ACE (Figure2 D)were significantly high in the low EA treated group than the high EA treated group. Phylogenetic diversity indicator PD_whole_tree was remarkably low than both the control group and the low EA treated group(Figure2 E). But no difference in observed species was found (Figure2 F).

The dominant phylum constituted by *Bacteroides*, *Firmicutes*, *Proteobacteria*, and *Verrucomicrobia* , likewise, *Akkermansia*, *Bacteroides*, *Blautia*, *Desulfovibrio*, *Helicobacter*, and *Intesinimonas* are the most abundant at the genus level (Figure2 G). Besides, the heat tree analysis leveraged the hierarchical structure of taxonomic differences between the control group and EA treated group. *Unidentified_Clostridiales* and *unidentified_bacteria* significantly altered in two branches as a comparison between the control group and the EA treated group (Figure2 H). Meanwhile, only *unidenfied_clostridiales* significantly altered when compared to the control group and the high EA treated group (Figure2 I).

Furthermore, heatmap analysis on the top 40 most-abundant genus was performed (Figure3 A). Notably, *Blautia*, *Roseburia*, *Lactobacillus* hold more abundance in the high EA treated group while *Faecalibaculum*, *Candidatus_Saccharimonas*, *Alloprevotella*, and *Lachnoclostridum*.et.al showed to be more abundant in the low EA treated group. Lefse analysis of the whole microbiome showed that differences among groups mainly occurred at the downstream of the family level(Figure3 B). In that case, the T-test analysis of microbial composition was also performed(Figure3 C), and results presented that *Helicobateraceae*, *unidentified_Clostridiales* increased while *Rikenellaceae* were reduced in the low EA treated group ($P < 0.05$). Only unidentified_Clostridiales were significantly increased in high EA treated groups.

3.3 Metabolic functions driven by different EA levels

PCA analysis based on metagenome showed no apparent separations among groups (Figure 4 A). *Carbohydrate metabolism*, *Membrane transport*, *Replication and repair*, *Translation*, *Amino acid metabolism*, *Energy metabolism*, *Nucleotide metabolism*, *Glycan biosynthesis and metabolism*, *Metabolism of cofactors and vitamins* and *Signal transduction* were the top ten most abundant pathways at KEGG level 2 (Figure4 B). Heatmap illustrated the composition of KEGG level 3 pathways that enriched in each group (Figure4 C). *Glycan biosynthesis*, *Metabolism of cofactors and vitamins*, and *Nucleotide metabolism* showed more richness in the high EA group. However, no statistically significant differences between the control group and high EA treatment were observed at KEGG level 3. But significant variations between the control group and the low

EA treated group were identified and that *Oxidative phosphorylation, Lipopolysaccharide biosynthesis, Arginine and proline metabolism, Folate biosynthesis* and *Biotin metabolism* were more abundant in the low EA group (Figure4 D).

3.4 Impacts of EA treatment on body weight and colonic morphology

EA treatments had no impacts on body weight, average daily food and water intake (**Figure 5**). Compared with the control group, the proximal colonic crypt depth of both EA treated groups showed significant reductions ($P < 0.0001$, **Figure5** F-H)) and villus/crypt ratio significantly increased in the high EA treated group ($P < 0.0001$). Meanwhile, EA treatments significantly increased the villus height and villus/crypt ratios of distal colon ($P < 0.05$).

3.5 Ethanolamine altered intestinal permeability and antimicrobial protein mRNA expression

The mRNA and protein expression of occludin in the low EA treated group were increased compared with those in control groups ($P < 0.001$, Figure6 A-D). Antimicrobial protein Reg3β, BD2, and MUC2 mRNA were significantly up-regulated in EA treated groups($P < 0.005$).Relative expression of BD1 was remarkably more significant in the low EA treated group than in the control group($P < 0.05$, **Figure**6 F).

3.6 Ethanolamine changed the production and mRNA expression of inflammation-related cytokines and Serum indicators

For mucosal inflammation-related cytokines in the colon, the concentration of IL1, IL6, IL17, TNFα, and INFγ showed a significant reduction in EA treated groups ($P < 0.01$). Conversely, sIgA was significantly up-regulated in both low and high EA treated groups (Table 1).

The concentration of serum ALT and AST were significantly down-regulated in the high EA treated group compared with the control group ($P < 0.05$, Figure7 A&B) and no differences in TBA and DAO concentration were found in this study (Figure7 C&D). The mRNA expression of IL1β showed a significant reduction in the EA treated groups, and the expression of IL6, IL10, IL22, sIgA and TNFα mRNA were significantly up-regulated ($P < 0.05$, E-L).

3.7 Ethanolamine promoted TLR4/MyD88 dependent signaling in inflamed colon tissues.

As the dramatic changes in microbiota discussed above, we further determine whether EA altered gut microbiota composition rely on TLR4/MyD88 dependent signaling. Compared with control group, the protein expression of TLR4 in LowEA and MyD88 in HighEA were significantly up-regulated (Figure8 A). The mRNA expression of MyD88 was up-regulated in the high EA treated group (Figure8 A). However, while TLR4 only showed a significant increase in the low EA treated group ($P < 0.05$, Figure8 C).

3.8 Ethanolamine increased the expression of TLR4 and occludin in the DSS-treated

organoid model.

To further determine the effects of EA on TLR4 expression and intestinal permeability, colonic organoids from intestinal crypts were directly derived from three male 8-week-old ICR mice for the establishment of DSS-treated organoid model (Figure9 A&B). The preliminary experiment showed that organoids could not survive in a 3000μM EA environment. In that case, ethanolamine treatment with 0μM, 100μM, and 500μM were performed in the DSS-treated organoid model. 500μM ethanolamine supplementation in the organoid growth medium significantly increased the surface area and budding rate of colonic organoids ($P < 0.05$, Figure8 C&D). TLR4 protein expression tended to be more significant in the 500μM EA treated group (Figure 9 G&H). The mRNA expression of TLR4 in 500μM ethanolamine treated group and MyD88 in both 100μM and 500μM ethanolamine treated group showed a significant increase (Figure 9 I-J). For mucosal permeability, occludin mRNA was significantly up-regulated in 500μM ethanolamine treated group (Figure9 K-L). The relative mRNA expression of all antimicrobial proteins, including Reg3β, BD1, BD2, and MUC2, were also detected on colonic organoids, and only Reg3β showed a significant up-regulation in 500μM ethanolamine treated group (Figure9 M).

Discussion

Nutrition signal to the host-microbiome interactions ultimately affect the pathological process and health outcomes[3-5, 15]. Dramatic alterations in gut microbiota and barrier dysfunction reflecting a different ecological microenvironment in IBD Patients and mice models compared with health conditions have been demonstrated by extensive works[1, 3-4, 6, 23]. Patients with Crohn's disease showed reduced diversity of fecal microbiota and held the gut microbiome that dominantly constituted by *Proteobacteria*, *Actinobacteria*, *Firmicutes*, and *Bacteroidetes*[32]. Dietary intervention with optimal dietary components such as fiber, short-chain fatty acids, and tryptophan has been proved to be able to reduce colonic inflammation and cell proliferation and shift the progression of IBD through the gut microbiota[3, 33]. Sphingolipids like PE and EA have been detected as the most differentially abundant metabolite in stool and intestinal tissue resections from IBD patients[3, 15]. Here, we tried to demonstrate the role of ethanolamine as an essential lipid signal in mediating host-microbial interactions and its impacts on colonic barrier functions and inflammation.

The present study showed that 500 μM EA increased microbial diversity. However, higher concentration of EA (3000μM) decreased microbial abundance. Gut microbiome dysbiosis in IBD has been identified as a decrease in microbial diversity and abundance due to a shift in the balance between commensal and potentially pathogenic bacteria[34]. These changes indicated that EA could change intestinal microbial compostion of the DSS-treated mice. The dominant phylum in EA treated groups constituted by *Bacteroides, Firmicutes, Proteobacteria, and Verrucomicrobia* , *Akkermansia, Bacteroides, Blautia, Desulfovibrio, Helicobacter.* A recent study highlighted the role of *Bacteroides*-derived sphingolipids in host-microbe symbiosis and inflammation, where IBD patients have decreased sphingolipid production by *Bacteroides*, but increased host-produced sphingolipid abundance in gut[15]. *Akkermansia*, *Bacteroides*, and *Blautia* are associated with the production of beneficial microbial-derived metabolites such as short-chain fatty acids that have

been proved to be a key regulator in IBD[3]. Studies have shown that short-chain fatty acids can inhibit histone deacetylases in colonocytes and intestinal immune cells to downregulate proinflammatory cytokines and induce apoptosis in cancer cell lines[1-2]. Ethanolamine can generate acetate[10], that may be responsible for the beneficial role of EA in altering the gut microbiota. Here, we further analyzed the metabolic functions of the gut microbiome via applying theTax4fun algorithm package[31]. Significant variations between the control group and the low EA treated group were identified, and *Oxidative phosphorylation*, *Lipopolysaccharide biosynthesis*, *Arginine and proline metabolism*, *Folate biosynthesis* and *Biotin metabolism* were more abundant in the low EA treated group. These metabolic changes are coincident with studies that reported beneficial impacts of dietary fiber intervention in IBD[3, 34]. These results may indicate that EA could shift the composition and metabolic functions of colonic microbiota to restore microbial dysbiosis.

In this study, EA decreased the proximal colon crypt depth and increased the distal villus height. Previous study showed that Gut microbiota, including *Escherichia*, *Enterococcus*, *Bacteroides*, and *Clostridium genera*, could promote colorectal carcinogenesis by increasing aberrant crypt foci induced by 1, 2-dimethylhydrazine[3]. Under health conditions, the mucus layer covers the whole epithelial surface, which confers the lubrication, hydration, and protection of the underlying epithelial cells and the epithelial barrier integrity of intestines[36-37]. Tight junction proteins like occludin and ZO1 also contribute to the regulation of intestinal permeability that physically against the invasion of gut bacteria[37]. Antimicrobial proteins like BD1, BD2, and Reg3 family are often secreted by Paneth cells to clear up the pathogens and promote epithelial regeneration following intestinal infection[2, 23, 25]. However, IBD patients often suffered from prolonged enteric inflammation that ultimately damages intestinal epithelia, and subsequently leads to increased intestinal permeability that causing pathogenic infections[35]. For instance, *Akkermansia* recently has been proved to be a probiotic that may be beneficial to the IBD therapy, and direct administration of *Akkermansia* has been demonstrated to alleviate obesity-related metabolic disturbances and increase Muc2 production in DIO-mice, thus improving mucus layer thickness and intestinal permeability[38-39]. In this study, EA supplementation increased the expression of occludin, Reg3β, BD2, MUC2, and BD1. These results were indicating that EA may improve colonic barrier functions via reducing gut permeability and increasing antimicrobial protein secretion.

IBD patients consistently suffered from chronic inflammation characterized by up-regulated proinflammatory cytokines such as IL1, IL6, IL17, TNFα, and INFγ that contribute to the establishment of tumor-associated immune microenvironment[14]. These proinflammatory cytokines are produced by CD4+ T helper (Th) lineage cells via IL12-Th1 and IL-23-Th17 pathways in IBD patients and mice with colitis[40-41]. Alterations in gut microbiota also have been demonstrated to be responsible for the regulation of Th1/Th17 immune response in IBD[2, 40]. Besides, sIgA up-regulated in the colon of IBD patients than that in healthy people[1]. Secretory IgA is generated by the combined function of plasma cells producing multimeric IgA and epithelial cells expressing pIgR, and it can protect the mucosal barrier against toxins and bacteria infections[42]. In this study, IL1, IL6, IL17, TNFα, and INFγ showed a significant reduction in EA treated groups. Conversely, sIgA was significantly up-regulated in EA treated groups. Further, IL12-Th1 and IL23-Th17 pathway-related cytokine gene expression were investigated. IL1β mRNA showed a significant reduction in EA treated groups. IL6, IL10, IL22, and sIgA mRNA were significantly up-regulated

in the high EA treated group. However, relative TNFα mRNA expression showed a significant rise in EA treated groups. These results indicated that EA treatments may alleviate colonic inflammation via down-regulating both IL-12-Th1 and IL23-Th17 pathways and increase the sIgA secretion. ALT and AST are liver-specific enzymes released into serum following acute liver damage[29]. Both IBD patients and mice models have been demonstrated to hold high serum AST and ALT concentrations as a result of inflammatory liver injury[43].In this research, both serum ALT and AST were significantly down-regulated in the high EA treated group in DSS-treated mice. These results indicated that EA may had a benefical impact on liver inflammation, further studies need to elucidate it.

To date, most EA signaling related researches were focused on bacterial utilization and CDP-EA pathway in PE synthesis[11, 17, 19-20]. Our previous study has demonstrated that ethanolamine could promote the proliferation of IPEC-J1 cells by regulating the mTOR signaling pathway and mitochondrial function[44]. Toll-like receptors (TLRs) have a vital role in mucosal immune responses to gut bacteria, and the TLR4 expression was always dramatically up-regulated in the intestines of IBD patients[21]. Myeloiddifferentiationfactor 88 holds its essential role in the regulation of innate gut immunity, and it is the direct downstream of TLRs and cytokine receptors[22]. Nutrient signals such as peptidoglycan and lipopolysaccharide can activate TLR4-MyD88 dependent or independent pathways to regulate the expression of antimicrobial proteins like the Reg3 protein family that ultimately reprogramme the gut microbiome in IBD[23-24]. Here, in the DSS-treated mice model, TLR4 protein was significantly up-regulated in EA treated groups, and MyD88 protein showed significantly up-regulated in the high EA treated group. However, MyD88 mRNA was up-regulated in the highEA group, while TLR4 only showed a significant increase in the low EA group. Crypt-derived colonic organoids can spontaneously generate crypt-villus like units and constituting by all types of intestinal cells. And so that colonic organoids hold the cellular and structural heterogeneity that highly coincident with the physiological nature of intestinal epithelium and much better than traditional cell lines in characterizing the immunology of intestinal barrier[37]. Hence, a DSS-induced colonic organoid inflammation model was established to verify these findings. Results showed that TLR4 protein expression tended to be more significant in the 500μM EA treated group. At the same time, TLR4 mRNA showed a significant increase in 500μM EA treated group.MyD88 mRNA expression was significantly up-regulated in both 100μM, and 500μM EA treated group. These results demonstrated that EA could exert impacts on the regulation of TLR4/MyD88 signals, and differences between mice model and organoid model may be caused by gut microbiota[3], and EA may mediate host-microbiome cross-talk via TLR4/MyD88 dependent signaling in the inflamed gut.

In conclusion, this research demonstrated that EA may alleviate colonic inflammatory immunoreactions and microbiome dysbiosis via TLR4/MyD88 dependent signaling. EA treatment improved intestinal barrier functions by up-regulating the expression of occluding and antimicrobial protein. EA treatment alleviated colonic inflammatory response by down-regulating related cytokines (IL1, IL6, IL17, TNFα, and INFγ) and increasing sIgA secretion. Results from both DSS-treated mice and DSS-treated colonic organoids indicated that EA may directly target the TLR4/MyD88 dependent pathway to mediate host-microbial interactions in intestinal inflammation.

Acknowledgments

Jian Zhou thanks professor Xiong, Wan, and Yin for their support and encouragement. Zhou, Xiong, and Yin thank Pan Huang for her technical support.

Funding

This project was supported by National Program on Key Basic Research Project (2017YFD0500504, 2016YFD0501201), the National Natural Science Foundation of China (31702127), Natural Science Foundation of Hunan Province (2018JJ1028) and the Young Elite Scientists Sponsorship Program by CAST (2018QNRC001). Research Foundation of Education Bureau of Hunan Province, China (18B476).

Supplemental Materials

See the file"Supplemental materials. docx"

References

1. Scaldaferri, F.; Gerardi, V.; Lopetuso, L. R.; Del Zompo, F.; Mangiola, F.; Boskoski, I.; Bruno, G.; Petito, V.; Laterza, L.; Cammarota, G.; Gaetani, E.; Sgambato, A.; Gasbarrini, A., Gut Microbial Flora, Prebiotics, and Probiotics in IBD: Their Current Usage and Utility. *Biomed Research International* **2013**.

2. Wong, S. H.; Yu, J., Gut microbiota in colorectal cancer: mechanisms of action and clinical applications. *Nat Rev Gastroenterol Hepatol* **2019,** *16* (11), 690-704.

3. Lavelle, A.; Sokol, H., Gut microbiota-derived metabolites as key actors in inflammatory bowel disease. *Nat Rev Gastroenterol Hepatol* **2020,** *17* (4), 223-237.

4. Cani, P. D.; Jordan, B. F., Gut microbiota-mediated inflammation in obesity: a link with gastrointestinal cancer. *Nat Rev Gastroenterol Hepatol* **2018,** *15* (11), 671-682.

5. Round, J. L.; Mazmanian, S. K., The gut microbiota shapes intestinal immune responses during health and disease. *Nat Rev Immunol* **2009,** *9* (5), 313-23.

6. Honda, K.; Littman, D. R., The microbiome in infectious disease and inflammation. *Annu Rev Immunol* **2012,** *30*, 759-95.

7. Ren, W.; Chen, S.; Yin, J.; Duan, J.; Li, T.; Liu, G.; Feng, Z.; Tan, B.; Yin, Y.; Wu, G.,

469 Dietary arginine supplementation of mice alters the microbial population and activates
470 intestinal innate immunity. *J Nutr* **2014,** *144* (6), 988-95.
471 8. Gao, J.; Xu, K.; Liu, H.; Liu, G.; Bai, M.; Peng, C.; Li, T.; Yin, Y., Impact of the Gut
472 Microbiota on Intestinal Immunity Mediated by Tryptophan Metabolism. *Front Cell Infect*
473 *Microbiol* **2018,** *8*, 13.
474 9. Hamer, H. M.; Jonkers, D.; Venema, K.; Vanhoutvin, S.; Troost, F. J.; Brummer, R. J.,
475 Review article: the role of butyrate on colonic function. *Aliment Pharmacol Ther* **2008,** *27* (2),
476 104-19.
477 10. Zhou, J.; Xiong, X.; Wang, K.; Zou, L.; Lv, D.; Yin, Y., Ethanolamine Metabolism in the
478 Mammalian Gastrointestinal Tract: Mechanisms, Patterns, and Importance. *Curr Mol Med*
479 **2017,** *17* (2), 92-99.
480 11. Wu, Y.; Chen, K. S.; Xing, G. S.; Li, L. P.; Ma, B. C.; Hu, Z. J.; Duan, L. F.; Liu, X. G.,
481 Phospholipid remodeling is critical for stem cell pluripotency by facilitating
482 mesenchymal-to-epithelial transition. *Sci Adv* **2019,** *5* (11).
483 12. Patel, D.; Witt, S. N., Ethanolamine and Phosphatidylethanolamine: Partners in Health
484 and Disease. *Oxid Med Cell Longev* **2017,** *2017*, 1-18.
485 13. Zhou, J.; Xiong, X.; Wang, K. X.; Zou, L. J.; Ji, P.; Yin, Y. L., Ethanolamine enhances
486 intestinal functions by altering gut microbiome and mucosal anti-stress capacity in weaned rats.
487 *Br J Nutr* **2018,** *120* (3), 241-249.
488 14. Lin, Y. C.; Lin, Y. C.; Chen, C. J., Cancers Complicating Inflammatory Bowel Disease. *N*
489 *Engl J Med* **2015,** *373* (2), 194-5.
490 15. Brown, E. M.; Ke, X. B.; Hitchcock, D.; Jeanfavre, S.; Avila-Pacheco, J.; Nakata, T.;

491 Arthur, T. D.; Fornelos, N.; Heim, C.; Franzosa, E. A.; Watson, N.; Huttenhower, C.; Haiser, H.
492 J.; Dillow, G.; Graham, D. B.; Finlay, B. B.; Kostic, A. D.; Porter, J. A.; Vlamakis, H.; Clish, C.
493 B.; Xavier, R. J., Bacteroides-Derived Sphingolipids Are Critical for Maintaining Intestinal
494 Homeostasis and Symbiosis. *Cell Host & Microbe* **2019,** *25* (5), 668-+.
495 16. Thiennimitr, P.; Winter, S. E.; Winter, M. G.; Xavier, M. N.; Tolstikov, V.; Huseby, D. L.;
496 Sterzenbach, T.; Tsolis, R. M.; Roth, J. R.; Baumler, A. J., Intestinal inflammation allows
497 Salmonella to use ethanolamine to compete with the microbiota. *Proc Natl Acad Sci U S A*
498 **2011,** *108* (42), 17480-5.
499 17. Ormsby, M. J.; Logan, M.; Johnson, S. A.; McIntosh, A.; Fallata, G.; Papadopoulou, R.;
500 Papachristou, E.; Hold, G. L.; Hansen, R.; Ijaz, U. Z.; Russell, R. K.; Gerasimidis, K.; Wall, D.
501 M., Inflammation associated ethanolamine facilitates infection by Crohn's disease-linked
502 adherent-invasive Escherichia coli. *EBioMedicine* **2019,** *43*, 325-332.
503 18. Kaval, K. G.; Singh, K. V.; Cruz, M. R.; DebRoy, S.; Winkler, W. C.; Murray, B. E.; Garsin,
504 D. A., Loss of Ethanolamine Utilization in Enterococcus faecalis Increases Gastrointestinal
505 Tract Colonization. *mBio* **2018,** *9* (3).
506 19. Anderson, C. J.; Clark, D. E.; Adli, M.; Kendall, M. M., Ethanolamine Signaling Promotes
507 Salmonella Niche Recognition and Adaptation during Infection. *PLoS Pathog* **2015,** *11* (11),
508 e1005278.
509 20. Moore, T. C.; Escalante-Semerena, J. C., The EutQ and EutP proteins are novel acetate
510 kinases involved in ethanolamine catabolism: physiological implications for the function of the
511 ethanolamine metabolosome in Salmonella enterica. *Mol Microbiol* **2016,** *99* (3), 497-511.
512 21. Cario, E.; Podolsky, D. K., Differential alteration in intestinal epithelial cell expression of

513 toll-like receptor 3 (TLR3) and TLR4 in inflammatory bowel disease. *Infect Immun* **2000,** *68*
514 (12), 7010-7.
515 22. Koliaraki, V.; Chalkidi, N.; Henriques, A.; Tzaferis, C.; Polykratis, A.; Waisman, A.; Muller,
516 W.; Hackam, D. J.; Pasparakis, M.; Kollias, G., Innate Sensing through Mesenchymal
517 TLR4/MyD88 Signals Promotes Spontaneous Intestinal Tumorigenesis. *Cell Reports* **2019,** *26*
518 (3), 536-+.
519 23. Chu, H.; Mazmanian, S. K., Innate immune recognition of the microbiota promotes
520 host-microbial symbiosis. *Nat Immunol* **2013,** *14* (7), 668-75.
521 24. Chaniotou, Z.; Giannogonas, P.; Theoharis, S.; Teli, T.; Gay, J.; Savidge, T.; Koutmani, Y.;
522 Brugni, J.; Kokkotou, E.; Pothoulakis, C.; Karalis, K. P., Corticotropin-releasing factor
523 regulates TLR4 expression in the colon and protects mice from colitis. *Gastroenterology* **2010,**
524 *139* (6), 2083-92.
525 25. Zhou, J.; Xiong, X.; Yin, J.; Zou, L.; Wang, K.; Shao, Y.; Yin, Y., Dietary Lysozyme Alters
526 Sow's Gut Microbiota, Serum Immunity and Milk Metabolite Profile. *Front Microbiol* **2019,** *10*,
527 177.
528 26. Zhai, Z.; Zhang, F.; Cao, R.; Ni, X.; Xin, Z.; Deng, J.; Wu, G.; Ren, W.; Yin, Y.; Deng, B.,
529 Cecropin A Alleviates Inflammation Through Modulating the Gut Microbiota of C57BL/6 Mice
530 With DSS-Induced IBD. *Front Microbiol* **2019,** *10*, 1595.
531 27. Miyoshi, H.; Stappenbeck, T. S., In vitro expansion and genetic modification of
532 gastrointestinal stem cells in spheroid culture. *Nat Protoc* **2013,** *8* (12), 2471-82.
533 28. Wen, Y. A.; Li, X.; Goretsky, T.; Weiss, H. L.; Barrett, T. A.; Gao, T., Loss of PHLPP
534 protects against colitis by inhibiting intestinal epithelial cell apoptosis. *Biochim Biophys Acta*

535 **2015,** *1852* (10 Pt A), 2013-23.

536 29. Zou, L.; Xiong, X.; Liu, H.; Zhou, J.; Liu, Y.; Yin, Y., Effects of dietary lysozyme levels on
537 growth performance, intestinal morphology, immunity response and microbiota community of
538 growing pigs. *J Sci Food Agric* **2019,** *99* (4), 1643-1650.

539 30. Xiong, X.; Zhou, J.; Liu, H.; Tang, Y.; Tan, B.; Yin, Y., Dietary lysozyme supplementation
540 contributes to enhanced intestinal functions and gut microflora of piglets. *Food Funct* **2019,** *10*
541 (3), 1696-1706.

542 31. Asshauer, K. P.; Wemheuer, B.; Daniel, R.; Meinicke, P., Tax4Fun: predicting functional
543 profiles from metagenomic 16S rRNA data. *Bioinformatics* **2015,** *31* (17), 2882-4.

544 32. Manichanh, C.; Rigottier-Gois, L.; Bonnaud, E.; Gloux, K.; Pelletier, E.; Frangeul, L.; Nalin,
545 R.; Jarrin, C.; Chardon, P.; Marteau, P.; Roca, J.; Dore, J., Reduced diversity of faecal
546 microbiota in Crohn's disease revealed by a metagenomic approach. *Gut* **2006,** *55* (2), 205-11.

547 33. O'Keefe, S. J. D.; Li, J. V.; Lahti, L.; Ou, J. H.; Carbonero, F.; Mohammed, K.; Posma, J.
548 M.; Kinross, J.; Wahl, E.; Ruder, E.; Vipperla, K.; Naidoo, V.; Mtshali, L.; Tims, S.; Puylaert, P.
549 G. B.; DeLany, J.; Krasinskas, A.; Benefiel, A. C.; Kaseb, H. O.; Newton, K.; Nicholson, J. K.;
550 de Vos, W. M.; Gaskins, H. R.; Zoetendal, E. G., Fat, fibre and cancer risk in African
551 Americans and rural Africans. *Nature Communications* **2015,** *6*.

552 34. Ni, J.; Wu, G. D.; Albenberg, L.; Tomov, V. T., Gut microbiota and IBD: causation or
553 correlation? *Nat Rev Gastroenterol Hepatol* **2017,** *14* (10), 573-584.

554 35. Fries, W.; Belvedere, A.; Vetrano, S., Sealing the Broken Barrier in IBD: Intestinal
555 Permeability, Epithelial Cells and Junctions. *Current Drug Targets* **2013,** *14* (12), 1460-1470.

556 36. Witten, J.; Samad, T.; Ribbeck, K., Selective permeability of mucus barriers. *Curr Opin*

Biotech **2018,** *52*, 124-133.

37. Bar-Ephraim, Y. E.; Kretzschmar, K.; Clevers, H., Organoids in immunological research. *Nat Rev Immunol* **2020,** *20* (5), 279-293.

38. Anhe, F. F.; Pilon, G.; Roy, D.; Desjardins, Y.; Levy, E.; Marette, A., Triggering Akkermansia with dietary polyphenols: A new weapon to combat the metabolic syndrome? *Gut Microbes* **2016,** *7* (2), 146-53.

39. Everard, A.; Belzer, C.; Geurts, L.; Ouwerkerk, J. P.; Druart, C.; Bindels, L. B.; Guiot, Y.; Derrien, M.; Muccioli, G. G.; Delzenne, N. M.; de Vos, W. M.; Cani, P. D., Cross-talk between Akkermansia muciniphila and intestinal epithelium controls diet-induced obesity. *P Natl Acad Sci USA* **2013,** *110* (22), 9066-9071.

40. Moschen, A. R.; Tilg, H.; Raine, T., IL-12, IL-23 and IL-17 in IBD: immunobiology and therapeutic targeting. *Nat Rev Gastroenterol Hepatol* **2019,** *16* (3), 185-196.

41. Galvez, J., Role of Th17 Cells in the Pathogenesis of Human IBD. *ISRN Inflamm* **2014,** *2014*, 928461.

42. Pabst, O.; Slack, E., IgA and the intestinal microbiota: the importance of being specific. *Mucosal Immunology* **2020,** *13* (1), 12-21.

43. Oliveira, G. R.; Teles, B. C. V.; Brasil, E. F.; Souza, M. H. L. P.; Furtado, L. E. T. A.; de Costro-Costa, C. M.; Rola, F. H.; Braga, L. L. B. C.; Gondim, F. D. A., Peripheral neuropathy and neurological disorders in an unselected Brazilian population-based cohort of IBD patients. *Inflammatory Bowel Diseases* **2008,** *14* (3), 389-395.

44. Yang, H.; Xiong, X.; Li, T.; Yin, Y., Ethanolamine enhances the proliferation of intestinal epithelial cells via the mTOR signaling pathway and mitochondrial function. *In Vitro Cell Dev*

Biol Anim **2016,** *52* (5), 562-7.

Table 1. Expression of inflammation-related cytokines driven by different EA levels

Cytokines	Control	LowEA	HighEA	P-value
pg/mg·pro	0μM	500μM	3000μM	
IL1	202.8±11.42^{a}	136.75±9.048^{b}	87.903±6.480^{c}	<0.001
IL6	150.8±8.595^{a}	110.9±11.29^{b}	71.59±4.911^{c}	<0.001
TNFα	1185±33.09^{a}	889.4±72.60^{b}	566.2±30.21^{c}	<0.001
IL17	53.87±2.941^{a}	48.30±2.184^{a}	40.78±2.533^{b}	0.003
INFγ	115.1±6.708^{a}	85.15±6.030^{b}	40.22±3.054^{c}	<0.001
sIgA	36.11±2.209^{b}	39.06±2.605^{ab}	45.18±1.935^{a}	0.022
IL10	575.4±15.93	635.0±37.34	602.0±30.64	0.364
IL22	54.23±1.963	52.88±2.895	52.66±3.367	0.913

a,b Values within a row with different superscript letters differ significantly at $p < 0.05$.

Figure 1. Ethanolamine treatments altered the colonic morphology of DSS-treated mice. A. DSS (3%) in drinking water was exploited in generating intestinal inflammation, and then different levels of ethanolamine were supplied in the same way. **B.** Ethanolamine treatment reduced the bodyweight of mice with colitis. **C-D.** Ethanolamine treatment did not affect average daily food and water intake. E. Both proximal and distal colon morphology of mice were investigated. **F-H**. Ethanolamine significantly reduced the crypt depth and crypt/villus ratio of the proximal colon. **I-K.** Ethanolamine increased the villus height and villus/crypt ratio of the distal colon.

Figure 2. Impacts of EA treatments on the colonic microbiome. A-B. Shannon and Simpson indicators for microbial diversity .**C-D.**Chao1 and ACE indicators for microbial abundance. **E.** The metric PD_whole_tree for phylogenetic diversity. **F.** Observed species in the microbiome. **G.**Top-ten most abundant phylum and genus of microbiota in both the control group and EA treated groups. **H-I.** Significantly altered bacteria driven by different EA levels. The heat tree analysis was applied to leverage the hierarchical structure of taxonomic classifications to quantitatively (using the median abundance) and statistically (using the non-parametric Wilcoxon Rank Sum test) depict taxonomic differences between microbial communities.

Figure 3. Microbial differences driven by different EA levels in the colon of DSS-treated mice. A. Genus composition of both the control group and EA treated groups. **B.** Lefse analysis of whole OTU in all groups (LDA score=2.0). **C.** Differences in microbial composition between control and EA treated groups at the genus level.

Figure 4. Metabolic functions of colonic microbiota driven by different EA levels in the DSS-treated mice model. A. PCA analysis of predicted KEGG pathways. **B.** Top-10 most abundant pathways at KEGG level-2.**C.**Composition of metabolic pathways of colonic microbiota at KEGG level-3. **D.** Differences in metabolic functions between control and EA treated groups at the KEGG level-3. Moreover, no statistically significant differences existed between the control

group and high EA treatment

Figure 5. EA treatments altered the colonic morphology of DSS-treated mice. A. DSS(3%) in drinking water was exploited in generating intestinal inflammation, and then different levels of EA were supplied in the same way. **B.** EA treatment reduced the bodyweight of mice with colitis.**C-D.**EA treatment did not affect average daily food and water intake. E. Both proximal and distal colon morphology of mice were investigated. **F-H**. EA significantly reduced the crypt depth and crypt/villus ratio of the proximal colon. **I-K.** EA increased the villus height and villus/crypt ratio of the distal colon.

Figure 6. Impacts of EA on mucosal permeability and antimicrobial protein mRNA expression. A -D. Protein and mRNA expression of occludin.E-H,mRNA expression of Reg3β, BD1, BD2and MUC2.

Figure 7. Impacts of EA on serum indicators and mRNA expression of cytokine-related genes. A -D. Impacts of EA on serum ALT, AST, TBA, and DAO. **E-L**.Relative mRNA expression of IL1β,IL6,IL10,IL22,IL17A,sIgA,TNFα and INFγ genes.

Figure 8. Impacts of EA on protein and mRNA expression of TLR4 and MyD88.

Figure 9. Impacts of EA on TLR-4 and Occludin expression on DSS-treat colonic organoids. A-B. Establishing of DSS(3%) treated the colonic organoid model **C-D**. Impacts of EA treatments on the surface area and budding efficiency of colonic organoids. **E-F**. Organoid numbers per well and DSS disrupted organoid ratio. **G-H**. TLR4 protein expression in DSS-treated organoids driven by different EA levels. **I-J.** Relative mRNA expression of TLR4 and MyD88 genes. **K.** Occludin mRNA expression. **L.** Occludin imaging of the control group and 500μM group. **M.** Relative mRNA expression of antimicrobial proteins, only Reg3β significantly increased in 500μM group.

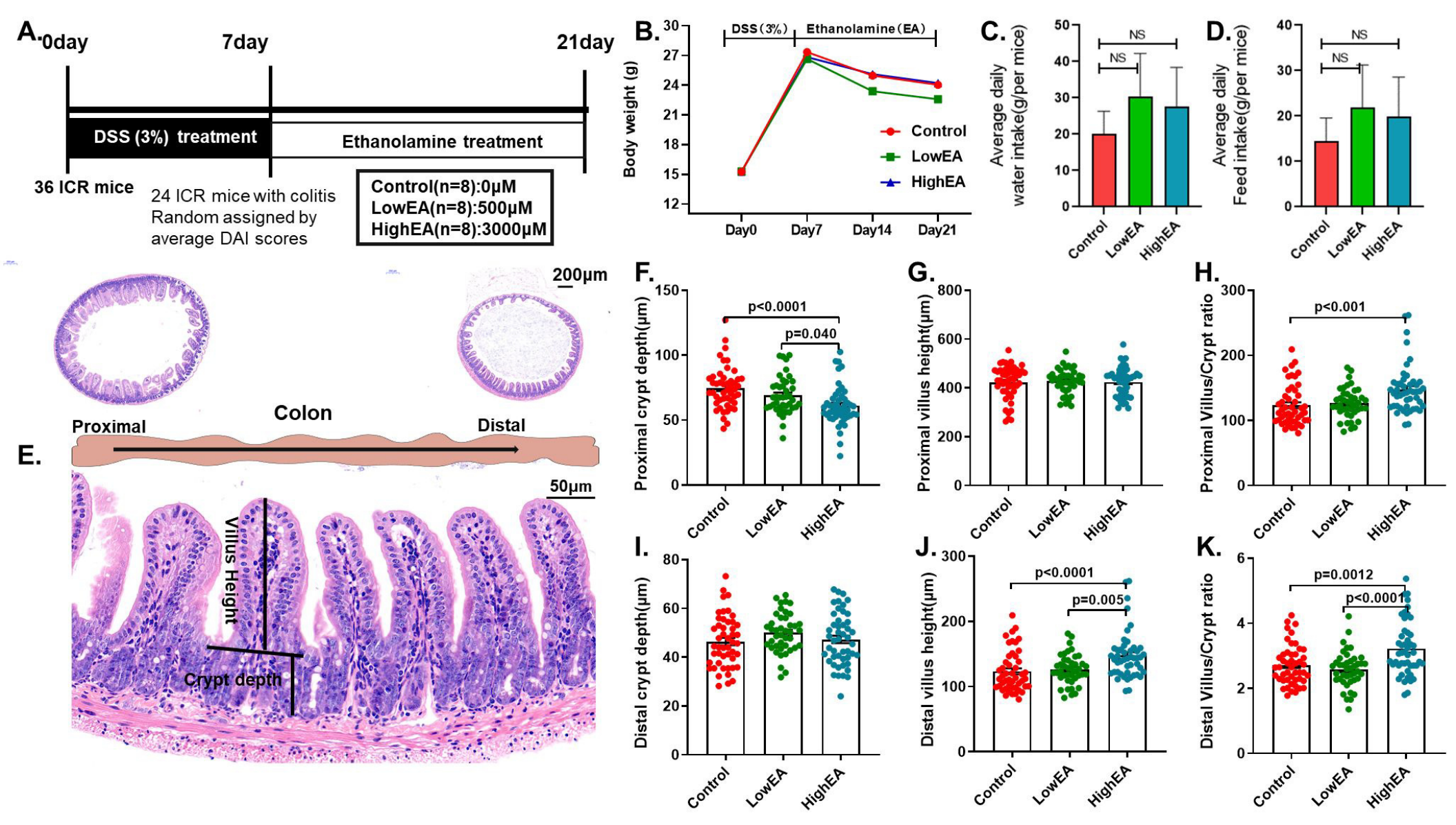
A.
0day
7day
21day
DSS (3%) treatment
Ethanolamine treatment
36 ICR mice
24 ICR mice with colitis
Random assigned by
average DAI scores
Control(n=8):0μM
LowEA(n=8):500μM
HighEA(n=8):3000μM
B.
DSS(3%)
Ethanolamine(EA)
Body weight (g)
Control
LowEA
HighEA
Day0
Day7
Day14
Day21
C.
Average daily water intake(g/per mice)
NS
NS
Control
LowEA
HighEA
D.
Average daily Feed intake(g/per mice)
NS
NS
Control
LowEA
HighEA
E.
200μm
Colon
Proximal
Distal
50μm
Villus Height
Crypt depth
F.
Proximal crypt depth(μm)
p<0.0001
p=0.040
Control
LowEA
HighEA
G.
Proximal villus height(μm)
Control
LowEA
HighEA
H.
Proximal Villus/Crypt ratio
p<0.001
Control
LowEA
HighEA
I.
Distal crypt depth(μm)
Control
LowEA
HighEA
J.
Distal villus height(μm)
p<0.0001
p=0.005
Control
LowEA
HighEA
K.
Distal Villus/Crypt ratio
p=0.0012
p<0.0001
Control
LowEA
HighEA

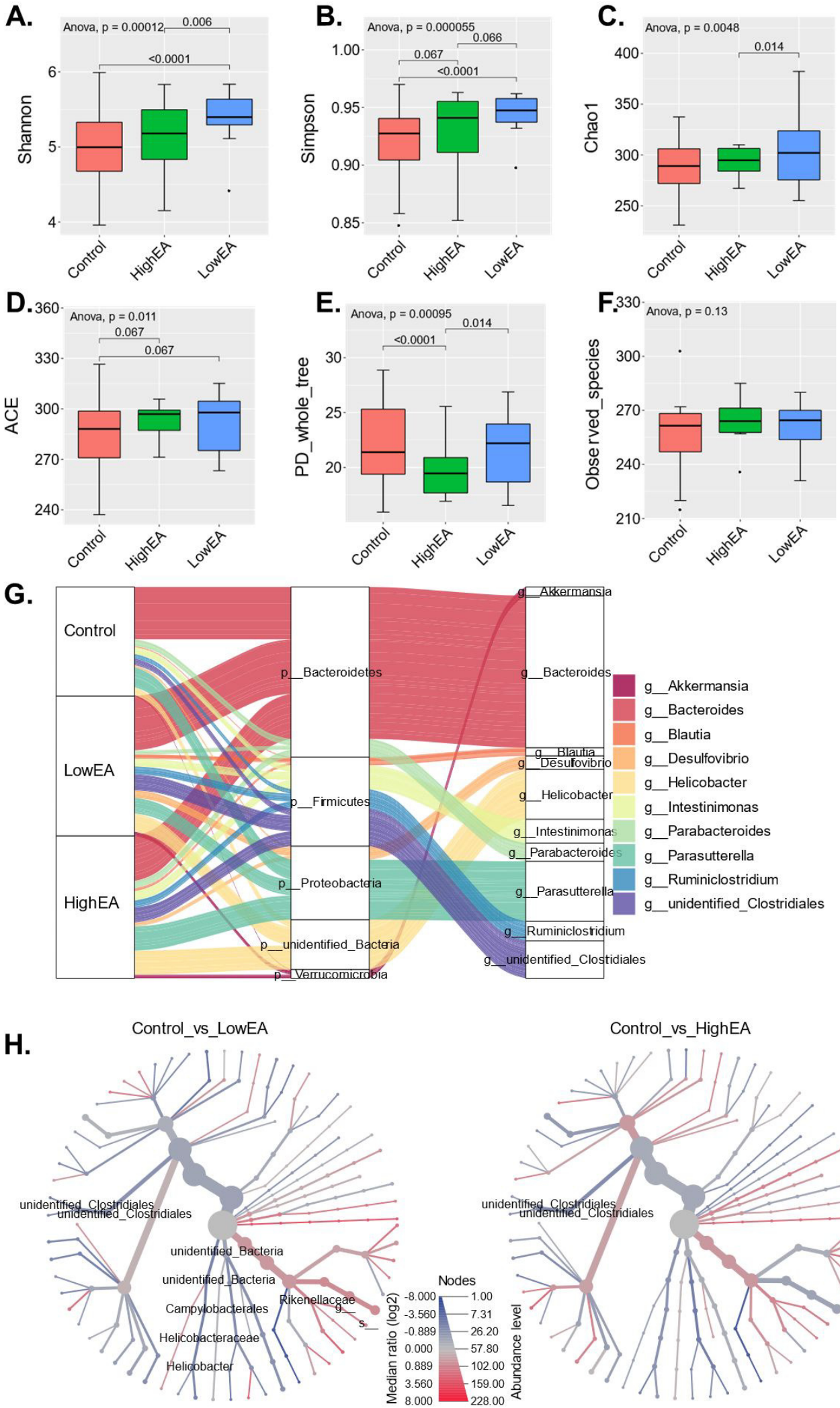
A.
Anova, p = 0.00012
0.006
<0.0001
Shannon
Control
HighEA
LowEA
B.
Anova, p = 0.000055
0.066
0.067
<0.0001
Simpson
C.
Anova, p = 0.0048
0.014
Chao1
D.
Anova, p = 0.011
0.067
0.067
ACE
E.
Anova, p = 0.00095
0.014
<0.0001
PD_whole_tree
F.
Anova, p = 0.13
Observed_species
G.
Control
LowEA
HighEA
p__Bacteroidetes
p__Firmicutes
p__Proteobacteria
p__unidentified_Bacteria
p__Verrucomicrobia
g__Akkermansia
g__Bacteroides
g__Blautia
g__Desulfovibrio
g__Helicobacter
g__Intestinimonas
g__Parabacteroides
g__Parasutterella
g__Ruminiclostridium
g__unidentified_Clostridiales
H.
Control_vs_LowEA
Control_vs_HighEA
unidentified_Clostridiales
unidentified_Bacteria
Campylobacterales
Rikenellaceae
Helicobacteraceae
Helicobacter
Nodes
Median ratio (log2)
Abundance level

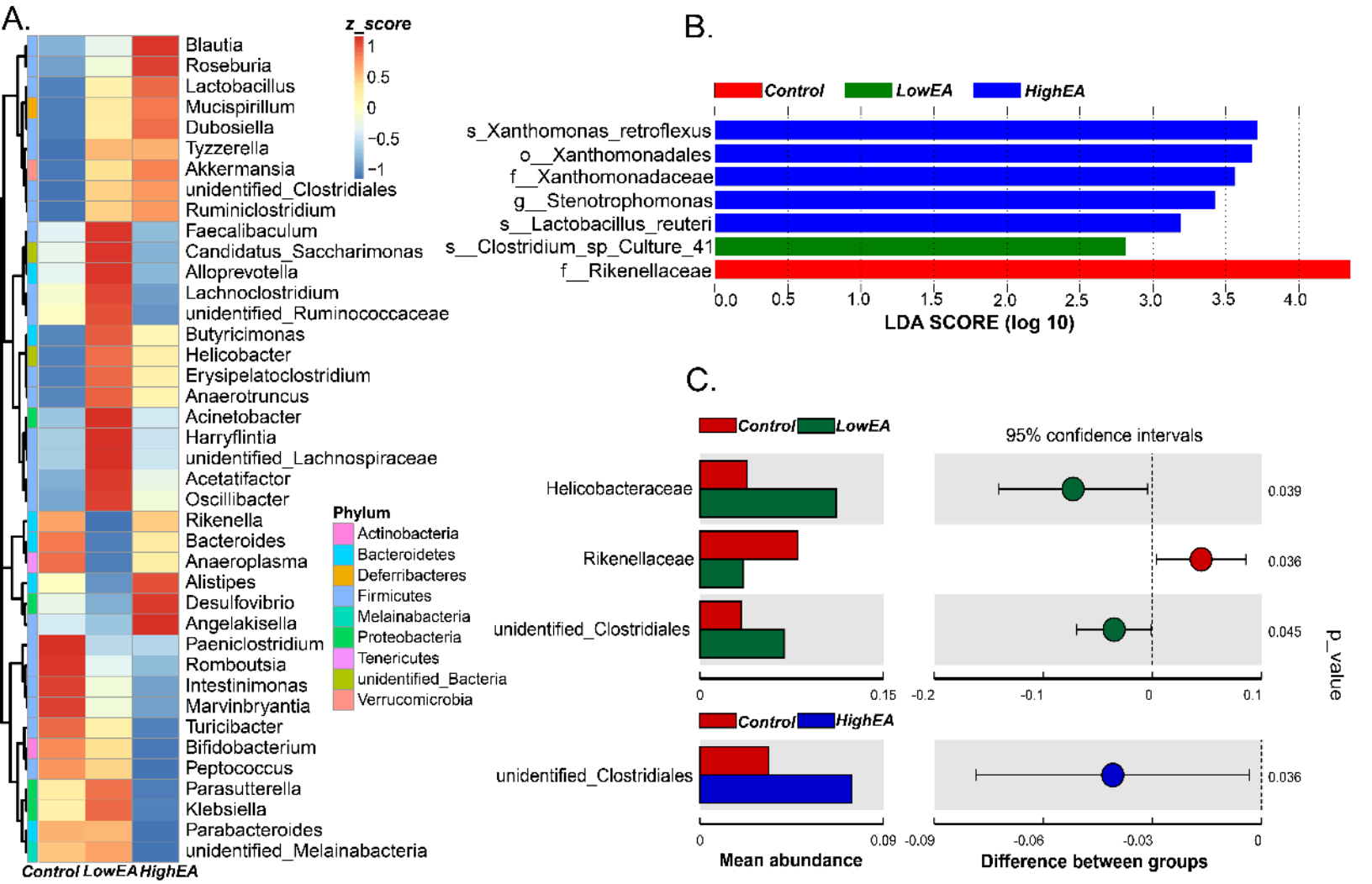
A.
z_score
1
0.5
0
−0.5
−1
Blautia
Roseburia
Lactobacillus
Mucispirillum
Dubosiella
Tyzzerella
Akkermansia
unidentified_Clostridiales
Ruminiclostridium
Faecalibaculum
Candidatus_Saccharimonas
Alloprevotella
Lachnoclostridium
unidentified_Ruminococcaceae
Butyricimonas
Helicobacter
Erysipelatoclostridium
Anaerotruncus
Acinetobacter
Harryflintia
unidentified_Lachnospiraceae
Acetatifactor
Oscillibacter
Rikenella
Bacteroides
Anaeroplasma
Alistipes
Desulfovibrio
Angelakisella
Paeniclostridium
Romboutsia
Intestinimonas
Marvinbryantia
Turicibacter
Bifidobacterium
Peptococcus
Parasutterella
Klebsiella
Parabacteroides
unidentified_Melainabacteria
Control LowEA HighEA
Phylum
Actinobacteria
Bacteroidetes
Deferribacteres
Firmicutes
Melainabacteria
Proteobacteria
Tenericutes
unidentified_Bacteria
Verrucomicrobia
B.
Control
LowEA
HighEA
s_Xanthomonas_retroflexus
o__Xanthomonadales
f__Xanthomonadaceae
g__Stenotrophomonas
s__Lactobacillus_reuteri
s__Clostridium_sp_Culture_41
f__Rikenellaceae
0.0 0.5 1.0 1.5 2.0 2.5 3.0 3.5 4.0
LDA SCORE (log 10)
C.
Control
LowEA
95% confidence intervals
Helicobacteraceae
Rikenellaceae
unidentified_Clostridiales
0.039
0.036
0.045
p_value
0 0.15
-0.2 -0.1 0 0.1
Control
HighEA
unidentified_Clostridiales
0.036
0 0.09
-0.09 -0.06 -0.03 0
Mean abundance
Difference between groups

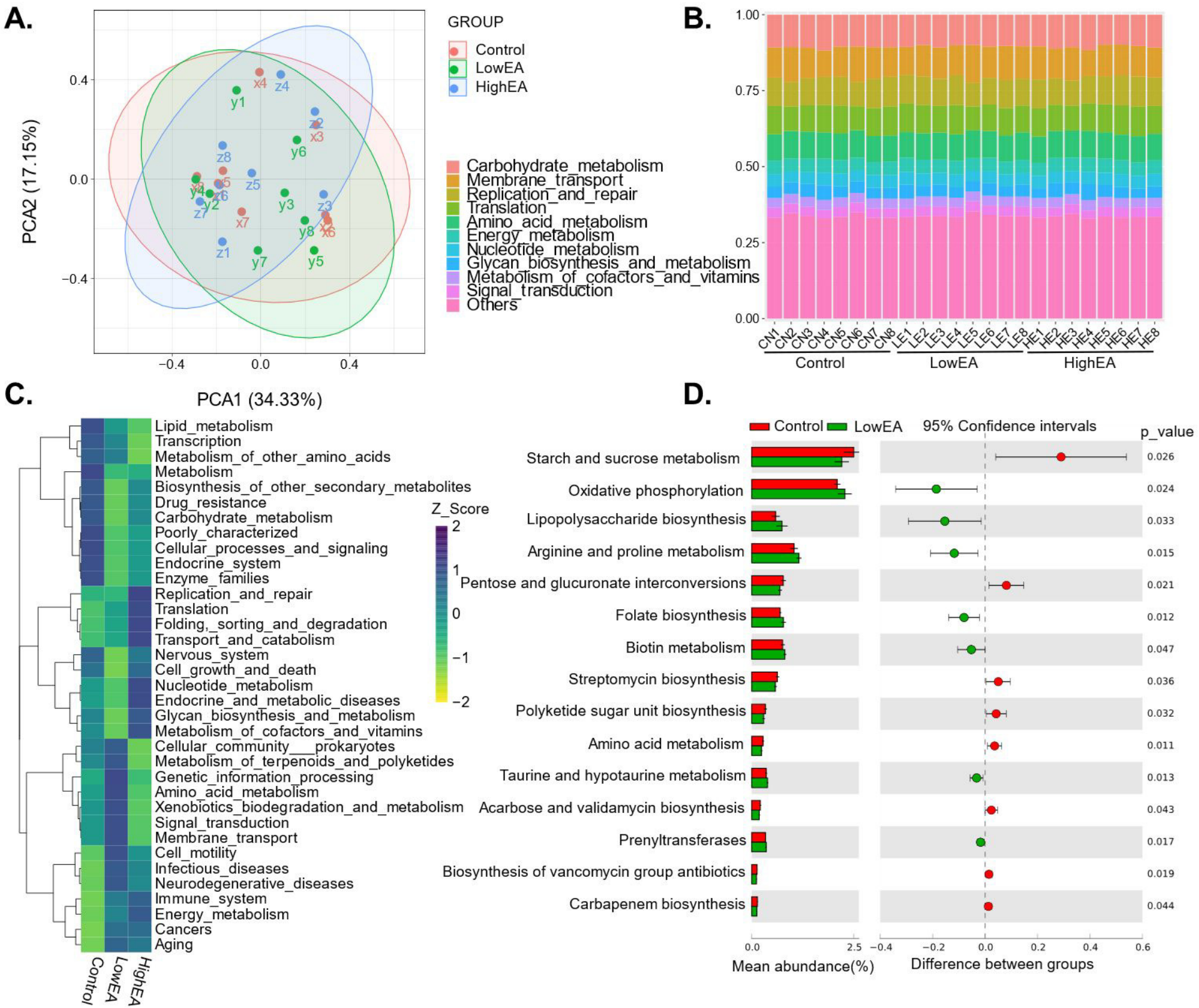
A.
GROUP
Control
LowEA
HighEA
PCA2 (17.15%)
PCA1 (34.33%)
B.
Carbohydrate_metabolism
Membrane_transport
Replication_and_repair
Translation
Amino_acid_metabolism
Energy_metabolism
Nucleotide_metabolism
Glycan_biosynthesis_and_metabolism
Metabolism_of_cofactors_and_vitamins
Signal_transduction
Others
Control
LowEA
HighEA
C.
Z_Score
Lipid_metabolism
Transcription
Metabolism_of_other_amino_acids
Metabolism
Biosynthesis_of_other_secondary_metabolites
Drug_resistance
Carbohydrate_metabolism
Poorly_characterized
Cellular_processes_and_signaling
Endocrine_system
Enzyme_families
Replication_and_repair
Translation
Folding,_sorting_and_degradation
Transport_and_catabolism
Nervous_system
Cell_growth_and_death
Nucleotide_metabolism
Endocrine_and_metabolic_diseases
Glycan_biosynthesis_and_metabolism
Metabolism_of_cofactors_and_vitamins
Cellular_community___prokaryotes
Metabolism_of_terpenoids_and_polyketides
Genetic_information_processing
Amino_acid_metabolism
Xenobiotics_biodegradation_and_metabolism
Signal_transduction
Membrane_transport
Cell_motility
Infectious_diseases
Neurodegenerative_diseases
Immune_system
Energy_metabolism
Cancers
Aging
Control
LowEA
HighEA
D.
Control
LowEA
95% Confidence intervals
p_value
Starch and sucrose metabolism
Oxidative phosphorylation
Lipopolysaccharide biosynthesis
Arginine and proline metabolism
Pentose and glucuronate interconversions
Folate biosynthesis
Biotin metabolism
Streptomycin biosynthesis
Polyketide sugar unit biosynthesis
Amino acid metabolism
Taurine and hypotaurine metabolism
Acarbose and validamycin biosynthesis
Prenyltransferases
Biosynthesis of vancomycin group antibiotics
Carbapenem biosynthesis
Mean abundance(%)
Difference between groups

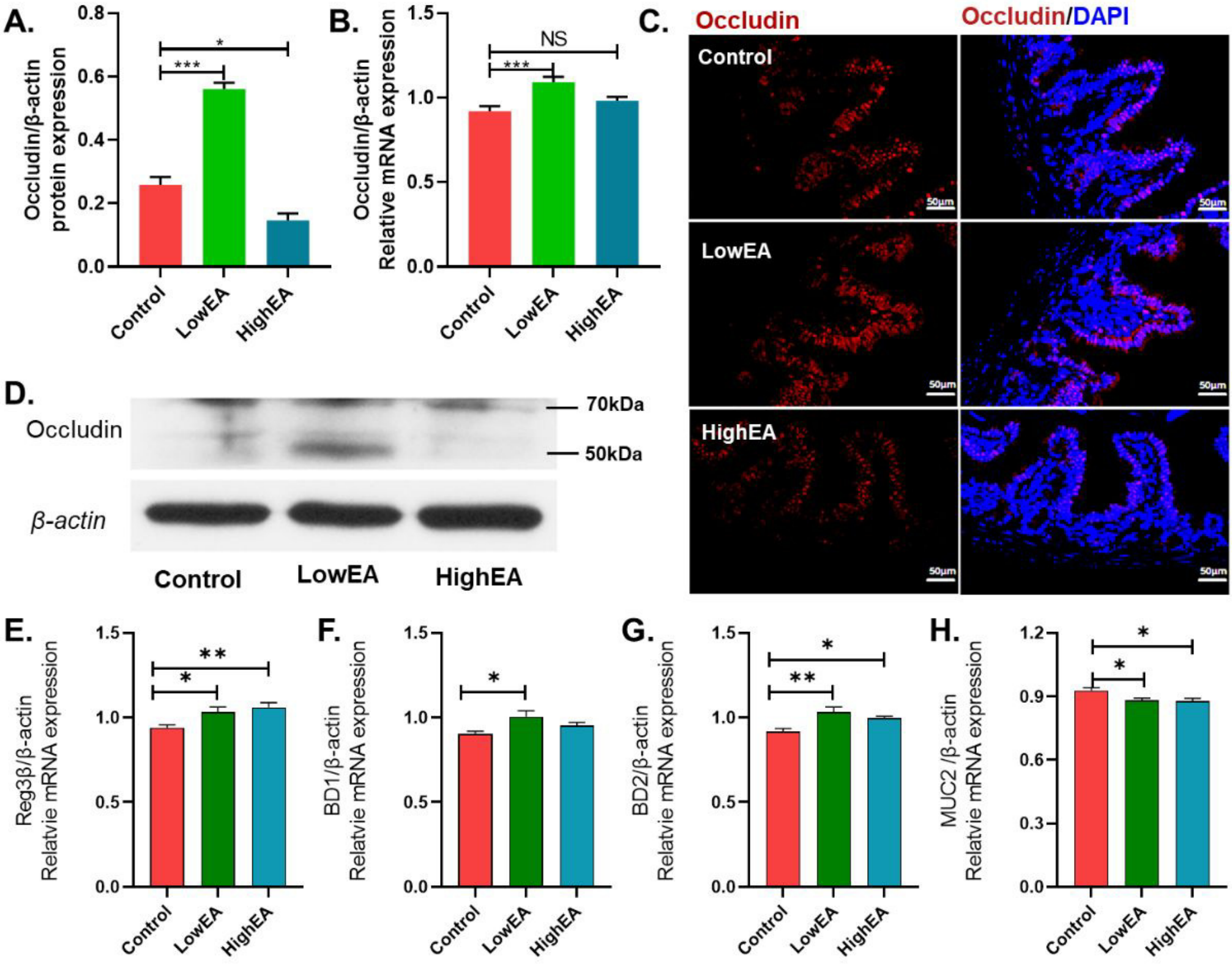
A.
Occludin/β-actin protein expression
0.8
0.6
0.4
0.2
0.0
*
***
Control
LowEA
HighEA
B.
Occludin/β-actin Relative mRNA expression
1.5
1.0
0.5
0.0
NS
***
Control
LowEA
HighEA
C.
Occludin
Occludin/DAPI
Control
LowEA
HighEA
50μm
D.
Occludin
β-actin
70kDa
50kDa
Control
LowEA
HighEA
E.
Reg3β/β-actin Relatvie mRNA expression
1.5
1.0
0.5
0.0
**
*
Control
LowEA
HighEA
F.
BD1/β-actin Relatvie mRNA expression
1.5
1.0
0.5
0.0
*
Control
LowEA
HighEA
G.
BD2/β-actin Relatvie mRNA expression
1.5
1.0
0.5
0.0
*
**
Control
LowEA
HighEA
H.
MUC2 /β-actin Relatvie mRNA expression
1.2
0.9
0.6
0.3
0.0
*
*
Control
LowEA
HighEA

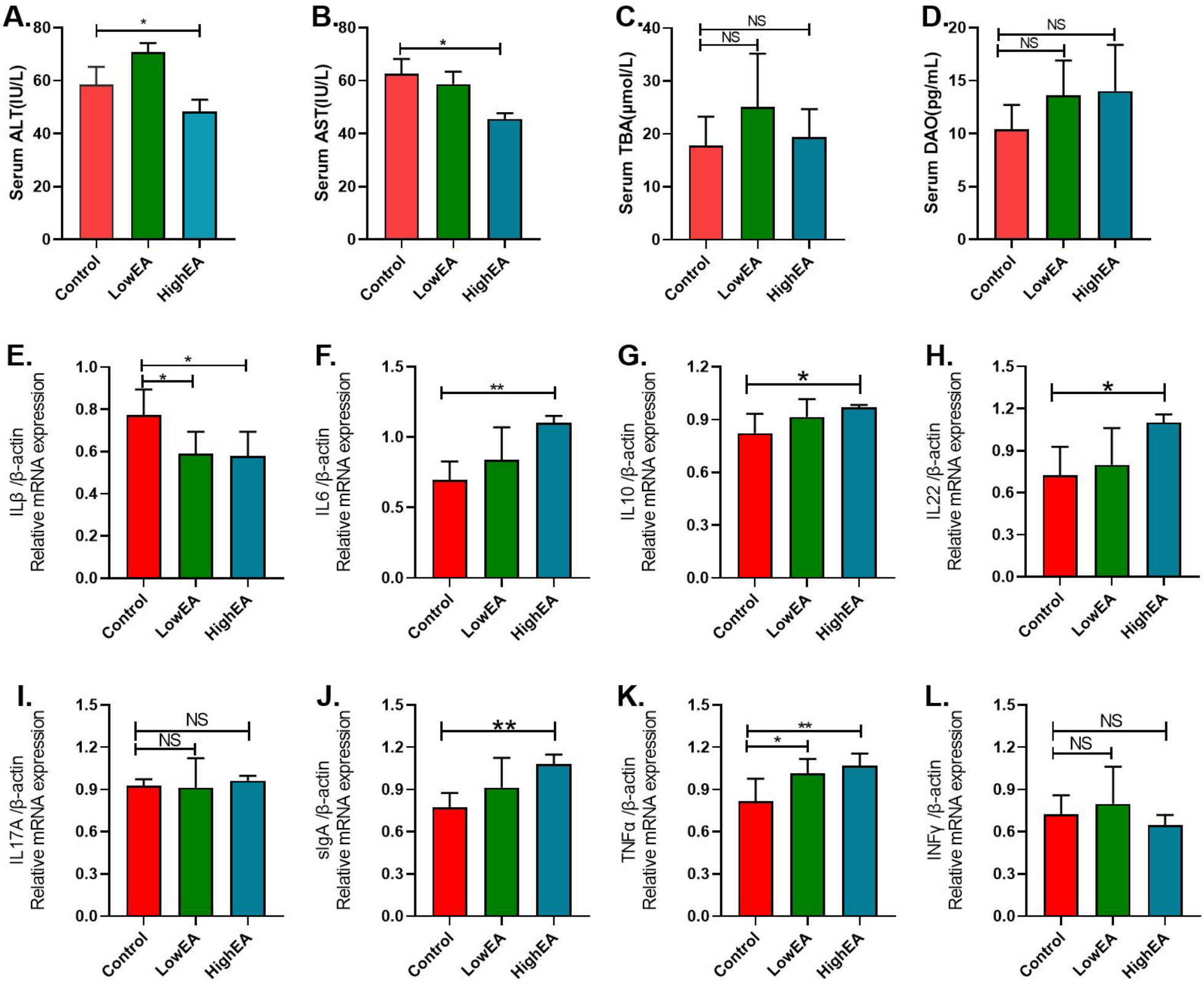
A.
Serum ALT(IU/L)
80
60
40
20
0
*
Control
LowEA
HighEA
B.
Serum AST(IU/L)
80
60
40
20
0
*
Control
LowEA
HighEA
C.
Serum TBA(μmol/L)
40
30
20
10
0
NS
NS
Control
LowEA
HighEA
D.
Serum DAO(pg/mL)
20
15
10
5
0
NS
NS
Control
LowEA
HighEA
E.
ILβ /β-actin
Relative mRNA expression
1.0
0.8
0.6
0.4
0.2
0.0
*
*
Control
LowEA
HighEA
F.
IL6 /β-actin
Relative mRNA expression
1.5
1.0
0.5
0.0
**
Control
LowEA
HighEA
G.
IL10 /β-actin
Relative mRNA expression
1.2
0.9
0.6
0.3
0.0
*
Control
LowEA
HighEA
H.
IL22 /β-actin
Relative mRNA expression
1.5
1.2
0.9
0.6
0.3
0.0
*
Control
LowEA
HighEA
I.
IL17A /β-actin
Relative mRNA expression
1.5
1.2
0.9
0.6
0.3
0.0
NS
NS
Control
LowEA
HighEA
J.
sIgA /β-actin
Relative mRNA expression
1.5
1.2
0.9
0.6
0.3
0.0
**
Control
LowEA
HighEA
K.
TNFα /β-actin
Relative mRNA expression
1.5
1.2
0.9
0.6
0.3
0.0
**
*
Control
LowEA
HighEA
L.
INFγ /β-actin
Relative mRNA expression
1.5
1.2
0.9
0.6
0.3
0.0
NS
NS
Control
LowEA
HighEA

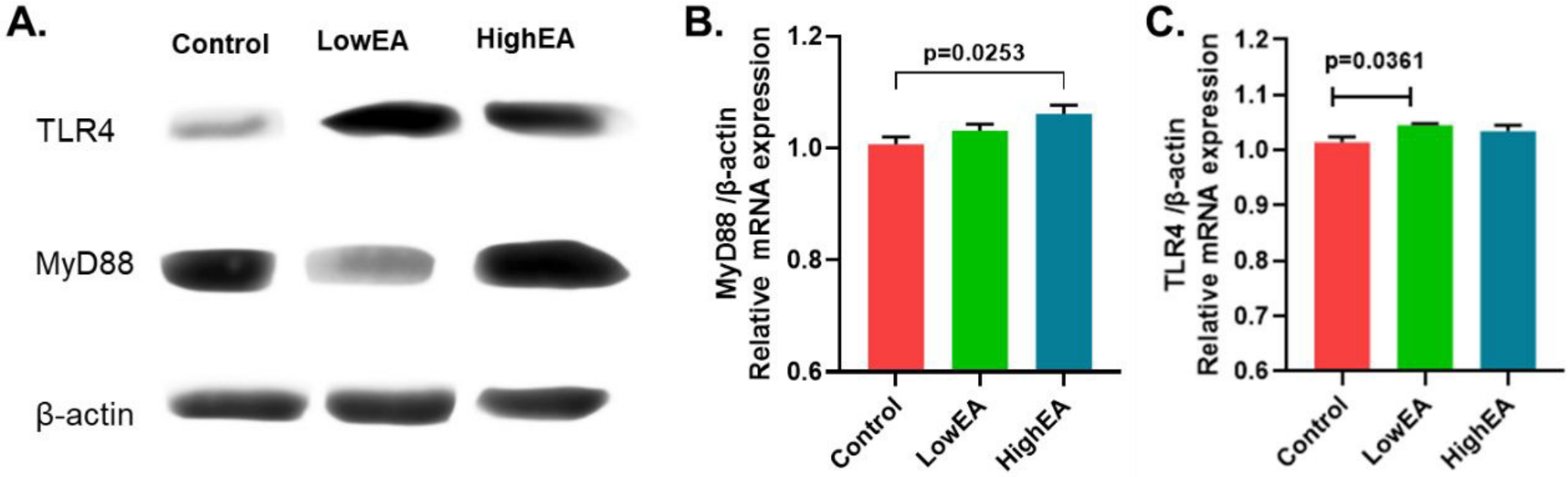
A.
Control
LowEA
HighEA
TLR4
MyD88
β-actin
B.
MyD88 /β-actin
Relative mRNA expression
p=0.0253
1.2
1.0
0.8
0.6
Control
LowEA
HighEA
C.
TLR4 /β-actin
Relative mRNA expression
p=0.0361
1.2
1.1
1.0
0.9
0.8
0.7
0.6
Control
LowEA
HighEA

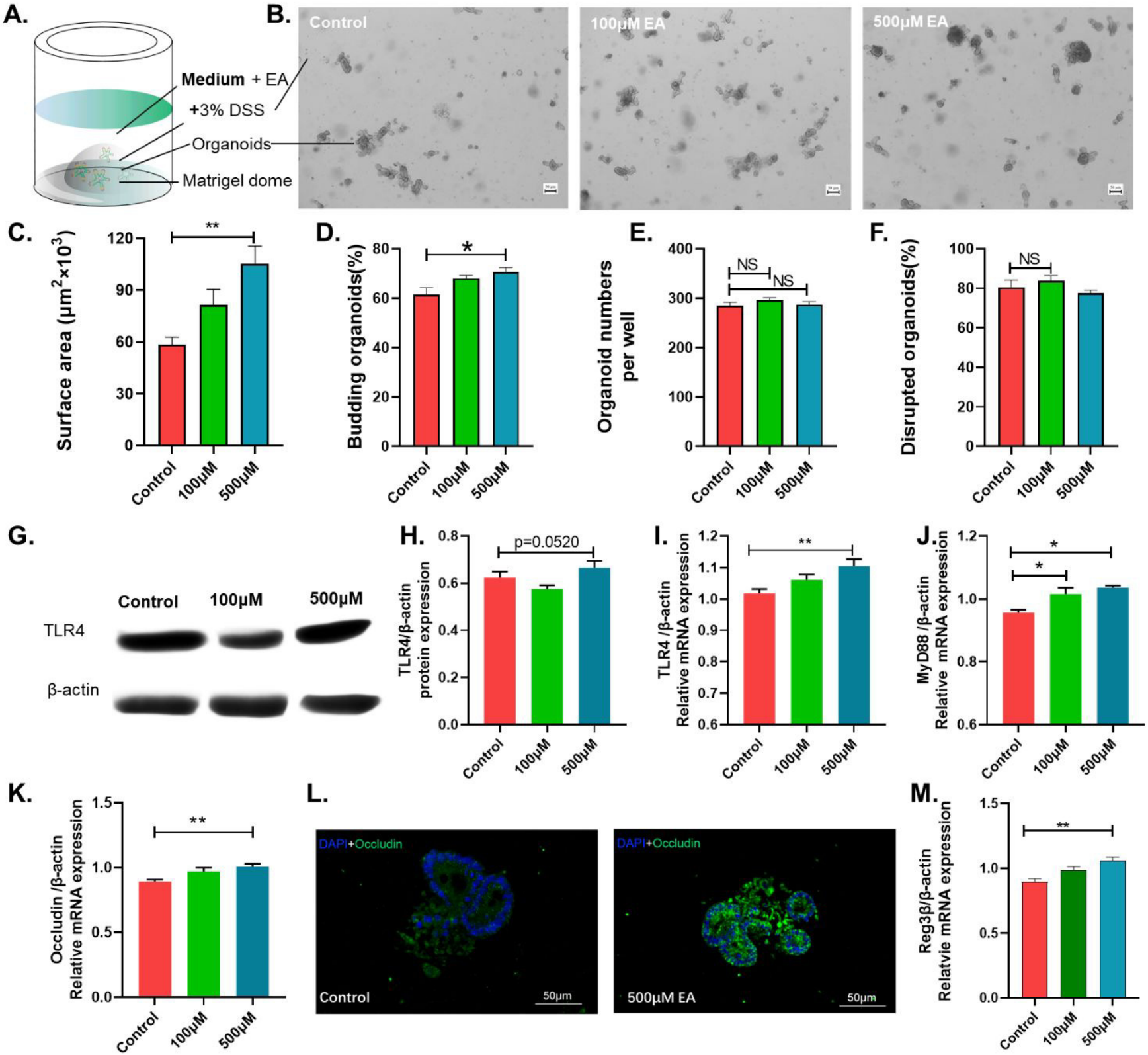
A.
Medium + EA
+3% DSS
Organoids
Matrigel dome
B.
Control
100μM EA
500μM EA
C.
Surface area (μm²×10³)
**
Control
100μM
500μM
D.
Budding organoids(%)
*
E.
Organoid numbers per well
NS
NS
F.
Disrupted organoids(%)
NS
G.
Control
100μM
500μM
TLR4
β-actin
H.
TLR4/β-actin protein expression
p=0.0520
I.
TLR4 /β-actin Relative mRNA expression
**
J.
MyD88 /β-actin Relative mRNA expression
*
*
K.
Occludin /β-actin Relative mRNA expression
**
L.
DAPI+Occludin
Control
50μm
DAPI+Occludin
500μM EA
50μm
M.
Reg3β/β-actin Relatvie mRNA expression
**